Performance of a Dual, Solid-State Intraoperative Probe System with ^{18}F, ^{99m}Tc, and ^{111}In

Raymond R. Raylman

Center for Advanced Imaging, Department of Radiology, West Virginia University, Morgantown, West Virginia

The use of tracer-avid radiopharmaceuticals and handheld, intraoperative, radiation-sensitive probes to localize areas of tumors promises to improve surgical treatments of cancer. Currently several β- and γ-ray-emitting radiopharmaceuticals are proposed for use in these procedures. Therefore, intraoperative-probe systems should be capable of optimum performance with several different radionuclides. The goal of this study was to evaluate the performance of a dual, solid-state probe with three of these radionuclides (^{18}F, ^{99m}Tc, and ^{111}In). **Methods:** The detector unit of the intraoperative-probe system used in this investigation consisted of a stack of two ion-implanted silicon detectors separated by 0.5 mm. The system could be operated in two modes: β optimized, in which the difference between the signals from the two detectors was calculated to correct the β signal for photon contamination, and photon-optimized mode, in which the signals were summed. Detection sensitivity and an index measuring β detection selectivity were measured in both acquisition modes with the three different radionuclides. The γ-ray detection sensitivity of a commercially available probe was measured with ^{99m}Tc and compared with the results with a solid-state probe. **Results:** β and photon emissions (γ-rays and annihilation photons) produced by all three radionuclides were detected by the probe. In β-optimized acquisition mode, the greatest β-detection sensitivity was achieved with ^{18}F; photon sensitivity was greatest for measurements with ^{111}In. The lowest detection sensitivities (β and photon) were obtained with ^{99m}Tc. With the probe system in γ-optimized mode, the greatest β and photon sensitivities were achieved with ^{18}F; the lowest were obtained with ^{99m}Tc. The γ-detection sensitivity measured with ^{99m}Tc in γ mode (5.59 $\pm$ 0.41 counts per second [cps]/kBq) compared surprisingly well with the results from the commercial probe (8.75 $\pm$ 0.47cps/kBq). **Conclusion:** The results from this investigation demonstrate the flexibility and versatility of the dual, solid-state probe system used in this study. These capabilities may be used to improve existing techniques or lead to new methods for performing radionuclide-guided surgeries.

Key Words: intraoperative probes; radionuclide-guided surgery; cancer

J Nucl Med 2001; 42:352–360

The use of intraoperative methods for guiding surgeries is a promising method for improving the effectiveness of the surgical treatment of cancer. The procedure begins before surgery with the administration of a tumor-avid pharmaceutical that is labeled, usually with a γ-ray-emitting radionuclide. During the subsequent surgical procedure, a handheld γ-ray-sensitive probe is used to survey regions of suspected disease to localize areas of increased tracer uptake and, therefore, sites of potential tumors. Monoclonal antibodies labeled with ^{125}I are perhaps the most commonly used radiopharmaceuticals in these procedures (*1–3*). In addition to ^{125}I-labeled agents, radiopharmaceuticals labeled with ^{111}In have also been used to guide cancer surgeries (*4–8*). For example, Muxi et al. (*4*) used ^{111}In-labeled anti-TAG72 monoclonal antibodies to guide the surgical removal of colorectal carcinomas. They reported a sensitivity of 82.1% for the detection of relatively large focal areas of tumor.

Davidson et al. (*9*) investigated the effect of background radiation on in vivo detection of colorectal tumors with a γ-ray probe used with an ^{111}In-labeled monoclonal antibody (ICR2). The detected ratios of tumor-to-normal tissue counts (T/N) measured by the probe during its placement in vivo above the tumors were compared to those measured using data from excised tumors (ex vivo) acquired with a well counter. The correlation between these two sets of data was poor ($r = 0.19$, $P < 0.52$). When the detected T/Ns measured with the probe above excised tumors were compared with the data from the well counter, the correlation was very good ($r = 0.84$, $P < 0.001$). The poor correlation calculated from the results acquired in vivo was caused by detection of background sources of penetrating radiation, which were absent in the probe measurements made outside the body. These results demonstrated that the effectiveness of radionuclide-guided cancer surgeries using ^{111}In-labeled radiopharmaceuticals is limited by poor target-to-background ratios (T/Ns) caused by detection of penetrating γ-rays emitted from distant sources of tracer uptake. To address this shortcoming, Saffer et al. (*10*) have constructed a coincidence probe to detect both of the γ-rays emitted by ^{111}In to reduce signal contamination originating from background sources of tracer uptake (*10*). This device is somewhat complex and requires a significant amount of signal-processing equipment, but it appears to effectively correct probe signals

TABLE 1
Radio-Emission Data for Three Radionuclides Used in This Study

Radionuclide	Emission type*	Frequency	Energy (keV)	Half-life	Initial amount (kBq)
[18]F	β^+	1.0	635.0†	110 min	2.3
[99m]Tc	γ	0.889	140.0	6.02 h	5.9
	ce	0.087	119.4		
[111]In	γ	0.905	171.3	2.8 d	5.1
	γ	0.940	245.4		
	CE	0.083	144.6		
	CE	0.050	218.7		
	X-ray	0.443	23.2		
	X-ray	0.236	22.9		
	X-ray	0.081	26.1		
	X-ray	0.024	26.6		
	X-ray	0.041	26.1		

*Maximum energy.
CE = conversion electrons.
Only emissions with energies greater than detector noise threshold (20 keV) and emission frequencies greater than 1% were listed.

for the presence of background radiation. Unfortunately, however, it is optimized for use only with [111]In.

Difficulties in tumor identification caused by the detection of background sources of radioactivity in vivo are not exclusive to procedures using [111]In. This phenomenon limits virtually all radionuclide-guided surgical procedures using γ-emitting radionuclides. To improve the effectiveness of these procedures, the use of radiopharmaceuticals labeled with β-particle (electron or positron)-emitting radionuclides has been proposed. The relatively short range of β particles in tissue (on the order of a few millimeters for most of the relevant radionuclides) might be a considerable advantage, because signal contamination from distant sources of tracer accumulation could be significantly reduced. Utilization of β-emitting radiopharmaceuticals, however, required the development of a new class of intraoperative probes. These devices were optimized for the detection of β particles and desensitized to background photons often associated with β-emitting radionuclides (11–16). Several of these probes have been designed for use primarily with the positron-emitting glucose analog ^{18}F-FDG. Studies using FDG with PET have demonstrated the excellent targeting of this radiotracer in several cancer types (17–21). For this reason, in addition to its emission of positrons, FDG is potentially an ideal radiotracer for use in radionuclide-guided surgeries. In addition to FDG, other radionuclides used to label cancer-imaging agents emit β particles, although in their most common applications the presence of the β particles is considered a nuisance. The radionuclide ^{111}In, for example, emits conversion electrons (145 and 219 keV), as well as two photons, (171 and 245 keV), which could be detected with a β probe (Table 1). Therefore, radiotracers labeled with ^{111}In could perhaps be used in conjunction with β-sensitive probes to guide surgeries.

Although radionuclide-guided surgery is a potentially valuable clinical technique, it has yet to be adopted routinely. One application of intraoperative probes, however,

that has begun to gain widespread acceptance is sentinel node biopsy (22–26). This technique usually uses a subcutaneous injection of the γ-ray-emitting radiopharmaceutical ^{99m}Tc-labeled sulfur colloid (Table 1) at the site of a known tumor. The radiotracer is transported to the lymph nodes responsible for drainage of the tumor site along lymphatic channels. Because of the size of the particles, some of the radioactive colloid becomes trapped in the lymph nodes. A handheld probe optimized for detection of γ-rays is then scanned over the area to localize the lymph nodes. Proper timing of the procedure allows identification of the sentinel node, which is removed and examined for the presence of cancer cells. If cancer is indeed found to be present in the sentinel node, the rest of the lymph node basin is dissected. Unlike techniques that use tumor-specific radiopharmaceuticals (such as FDG), sulfur colloid is nonspecific. Its presence in a lymph node does not imply the presence of cancer cells. Thus, the goal of the method is only to detect the sentinel node. Although specialized γ probes have been designed for sentinel node biopsy, it may be possible to use some β probes to effectively detect γ-rays emitted by [99m]Tc. The goal of this investigation was to evaluate the detection performance of a dual, solid-state probe system when used with the predominantly γ-ray-emitting radionuclides ^{99m}Tc and ^{111}In and with the β-particle-emitting radionuclide [18]F.

MATERIALS AND METHODS

Detector

The detector unit of the intraoperative β-probe system used in this work consisted of a stack of two ion-implanted silicon detectors (IISDs) incorporated into a single, compact unit (12). This design allowed for the correction of background photon flux by using the second detector in the stack as a monitor to estimate the amount of photon contamination present in the β signal detected by the first detector. The first detector was of sufficient thickness to absorb most of the β particles emitted by the radionuclides used

in this study. Thus, the rear IISD was bombarded by a pure photon flux representative of the photon flux component striking the first detector. The signal from the rear detector (scaled by a weighting factor to account for solid angle differences between the two detectors) was subtracted from that of the front detector to produce an estimate of the pure β signal. Each IISD had a circular active area of 50 mm^2 (diameter = 8 mm) and a 0.5-mm-thick depletion layer.

Electronics

The pulses from each of the IISDs were amplified and shaped by a preamplifier–amplifier combination. The variable-amplitude shaped pulses produced by each channel of electronics were pulse-height analyzed with a separate set of discriminator electronics located in the power- and pulse-processing module. The magnitude of each pulse was compared to a user-selected threshold voltage supplied by a laptop computer. The energy threshold for each detector was set at the detector noise level (20 keV), as recommended by the manufacturer. Each of the two discriminator channels produced transistor-to-transistor logic (TTL) pulses that were transmitted to a laptop computer for event counting. Power for the bias supply, preamplifiers, amplifiers, and discriminators was provided by two rechargeable 12-V batteries housed in the power- and pulse-processing module.

Probe Enclosure

The stacked IISD unit was housed in the tip of the intraoperative probe. The tip had an outer diameter of ~17.5 mm and a length of 19 mm. The front face of the tip was covered with a thin piece of aluminized Mylar. Electrical connections from the detectors to the electronics boards located in the probe handle were routed through a curved stainless steel tube connecting the probe tip and handle. The distances from detectors to the preamplifiers were ~7 cm. The variable-height pulses produced by the amplifiers were transmitted to the power- and pulse-processing module through ~120 cm of shielded, multiconductor cable. Sealed, watertight connectors were used to reduce the potential for electrical shock during use in surgery.

Data Acquisition Hardware

Both channels of pulse-height-discriminated data (TTL pulses) were transmitted through a 50-conductor ribbon cable to a laptop computer (Latitude CPi 233; Dell Computer Co.). The two channels of pulses were counted using a DAQCard-1200 PCMCIA card (National Instruments, Inc.) resident in the laptop. Each of the two counters had 16-bit resolution and a maximum source frequency of 8 MHz. The data acquisition card also had two analog output channels (digital-to-analog conversion [DAC]) and eight single-ended input channels (analog-to-digital conversion [ADC]).

Data Acquisition Software

Operation of the data acquisition hardware was controlled with software written using the LabVIEW graphical programming environment (National Instruments, Inc.). The length of the counting period was variable and user selectable. In addition, the user had the choice of acquiring data using one of two event-processing modes: β-particle-optimized or γ-ray-optimized mode. In β-optimized mode, the counts recorded from channel 2 (the photon monitor), weighted by a correction factor accounting for solid-angle differences, were subtracted from the counts acquired for channel 1 (β plus photon monitor). Thus, much of the photon contamination present in the β signal was removed. In γ-optimized

mode, the counts from channel 2, weighted by the correction factor, were added to the counts from channel 1. Summing the signals enhanced sensitivity to photon events. In either mode the processed counting rate, as well as the counting rate for each channel, was displayed on the user interface screen. The processed probe counts were also continuously plotted (in real time) on a large scrolling graph displayed on the interface screen. The operator had the option of saving the counting-rate data to an Excel-formatted file for subsequent analysis. Additionally, the lower energy threshold level used for pulse-height discrimination was selected using the computer interface.

Probe Performance Tests

The performance of the probe when used with each of three radionuclides (^{18}F, ^{99m}Tc, and ^{111}In) was characterized by measuring β and photon detection sensitivity in both β-particle-optimized and γ-ray-optimized detection modes. Additionally, a parameter measuring the rejection of background photon events, called the selectivity index (SI), was calculated using these data.

Sensitivity Measurements. One of the most common parameters used to evaluate the performance of intraoperative probes is detection sensitivity. Before performing the sensitivity measurements, however, the weighting factor used to account for solid-angle differences between the two IISDs was determined. The tip of the probe was positioned 1 mm above an 8-mm-diameter disk of thin absorbent paper containing 37 kBq (1 μCi) ^{18}F. The disk was then covered with a 1.0-mm-thick piece of stainless steel. This amount of stainless steel was sufficient to totally absorb all of the positrons emitted by ^{18}F. Thus, the detector unit was bombarded with a pure flux of penetrating 511-keV annihilation photons. Fifty samples, each with a duration of 10 s, were acquired. For each sample, the ratio of the counting rate recorded from the first detector to the second detector was calculated and defined as the correction-weighting factor for this source geometry. The mean of the 50 weighting factors was calculated and used for all of the subsequent measurements.

^{18}F (2.3 kBq [63 nCi]) was placed on a second 8-mm-diameter disk positioned 1 mm below the detector tip. The complete experimental set-up is shown in Figure 1. To measure the photon detection sensitivity, a 1-mm-thick piece of stainless steel was used to cover the disk. The counting rate data were corrected for absorption of a small fraction of the photon flux absorbed in the stainless steel. Positron sensitivity was measured by removing the positron-absorbent sheet of stainless steel. For each set of data, forty 5-s samples were obtained. The mean and SD counting rate for each dataset were then calculated. Data were acquired in both β- and γ-optimized acquisition modes. Subsequent datasets were periodically obtained in an identical fashion at later time points as the ^{18}F decayed. The probe counting rate was measured as a function of source strength over ~8 h. The amount of radioactivity in the disk ranged from 2.3 kBq (63 nCi) to 141 Bq (3.8 nCi) over the length of the experiment. The mean counting rate for each measurement was plotted as a function of source activity. The β and photon data were fit to straight lines using a weighted, least-square algorithm. The slopes of the lines were reported as measures of β-particle and annihilation-photon detection sensitivities. This procedure was repeated with each of the other two radionuclides, with the exception that initial amounts and duration of the experiment were tailored to the individual radionuclide (Table 1). Another exception to the procedure was the acquisition of additional photon detection sensitivity data with ^{99m}Tc, using a second
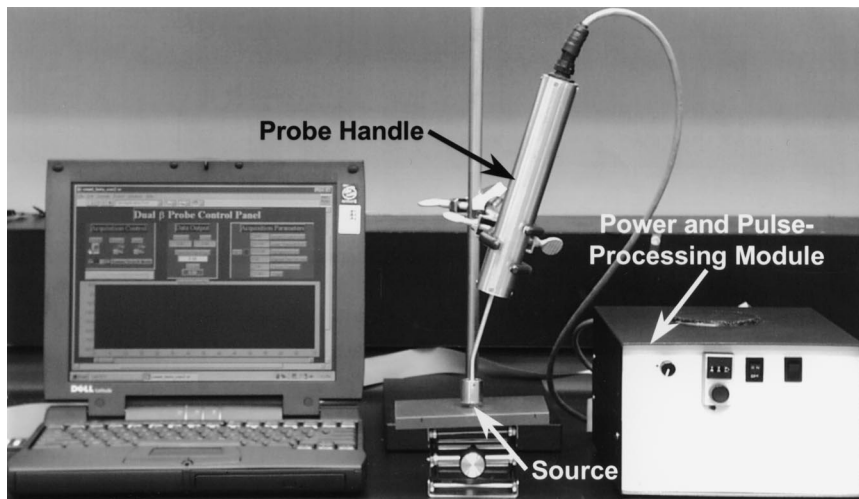
FIGURE 1. Experimental apparatus. Significant parts of setup are labeled.

probe. This probe, a Radiation Monitoring Devices, Inc. (RMD, Inc.) model GGS Navigator, is optimized for use with ^{99m}Tc and is currently used to guide sentinel node biopsies at our institution.

Selectivity Measurements. The ability to preferentially detect β particles is an important characteristic of a successful intraoperative β probe, given that in most uses either annihilation photons or γ-rays will accompany the β-particle flux. The capability of the β probe to correct for the presence of background photons produced by the three radionuclides tested was gauged by calculation of the selectivity index (SI), given by the equation (*12*):

$$SI = \frac{(S_\beta - S_\gamma)}{S_\beta} = \frac{(S_{\beta+\gamma} - S_\gamma - S_\gamma)}{S_{\beta+\gamma} - S_\gamma} = 1 - \frac{S_\gamma}{S_{\beta+\gamma} - S_\gamma} = 1 - \frac{S_\gamma}{S_\beta}.$$

S_β is the pure β sensitivity, S_γ is the pure photon sensitivity, and $S_{\beta+\gamma}$ is the combined, uncorrected β + photon sensitivity. The β- and photon-detection sensitivities previously measured were used to perform calculations of SI. The closer the index is to unity, the more effective the system was in correcting the β signal for the presence of photon contamination.

RESULTS

Figures 2–4 show the results of the β- and photon-sensitivity measurements performed with ^{18}F, ^{99m}Tc, and ^{111}In, respectively. Plots of counting rate as a function of source strength acquired in β mode and γ mode are shown. Detection sensitivities calculated from these curves are summarized in Table 2. For data acquired in β-optimized mode, the β-detection sensitivity was greatest for the pure positron-emitting ^{18}F and was lowest for ^{99m}Tc, which emits a small number of conversion electrons per decay. Photon detection sensitivity was greatest for ^{111}In and smallest for ^{18}F. These results were, mostly, the result of lower-energy γ-rays emitted by ^{111}In, which had a higher interaction cross-section in silicon compared with photons produced by the annihilation of positrons emitted by ^{18}F. When data were acquired in γ mode, measurements with ^{18}F produced the highest photon sensitivity, whereas measurements with ^{99m}Tc resulted in the lowest. The results for photon detection

sensitivity measured with the RMD, Inc. Navigator probe, a device optimized for use with ^{99m}Tc, compared surprisingly well with the sensitivity results for the probe system operated in γ mode. These results show that the Navigator was only ~1.56-fold more sensitive to the photons emitted by ^{99m}Tc than the dual, solid-state probe. The nonzero y-intercepts calculated from the linear fits performed on the curves in Figures 2–4 were caused by statistical noise in the counting rate data. Finally, the selectivity indices calculated for the two acquisition modes are show in Table 3. These results demonstrate that, as expected, the greatest rejection of background photon events was achieved in β acquisition mode. As with detection sensitivity, the magnitudes of the SIs were related to the type and energy of the particles emitted by the individual radionuclide.

DISCUSSION

The effectiveness of radionuclide-guided surgeries has been hampered by the relatively low tumor uptake of many of the γ-emitting radiopharmaceuticals currently applied to these procedures. Difficulties in localizing tumors caused by low uptake are exacerbated by reduction of detected T/Bs caused by detection of background sources of γ radiation. The use of radiopharmaceuticals labeled with β-emitting radionuclides promises to improve detected T/Bs, and therefore facilitate accurate localization of tracer-avid regions. The radiopharmaceutical most commonly proposed for use in β-emitting-radionuclide–guided surgery is ^{18}F-FDG. The very good tumor-targeting capabilities of this glucose analog make it an excellent candidate for this application.

The results shown in Figure 2, Table 2, and Table 3 demonstrate the very good performance of this probe system when used with ^{18}F. The detected β sensitivity measured in β-optimized mode is a factor of ~2 greater than another background-compensated probe designed by Daghighian et al. (*11*). The photon-detection sensitivity measured in β mode was very small because of the effective
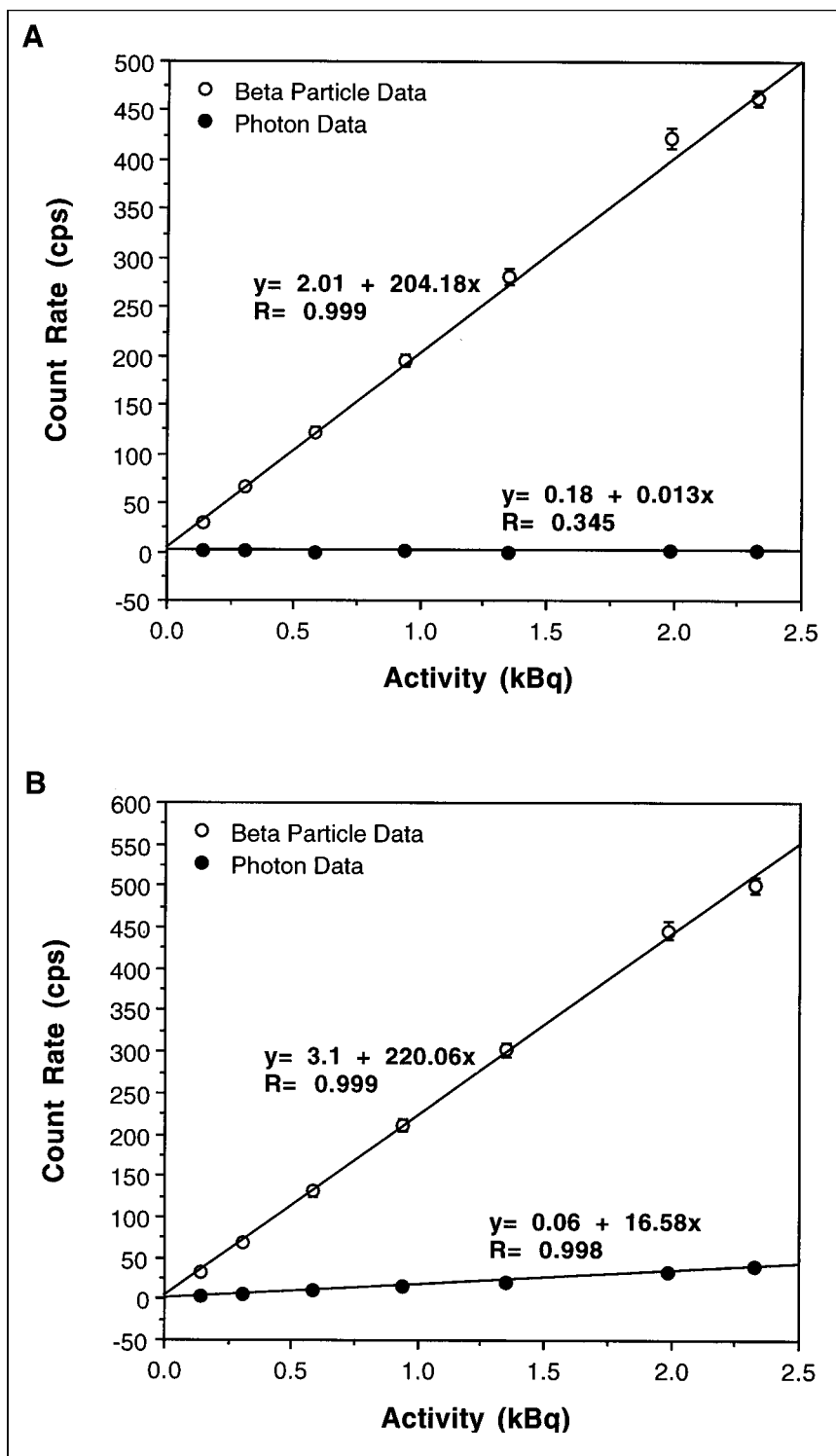
FIGURE 2. Results of sensitivity measurements for ^{18}F for two different acquisition modes. (A) β mode. (B) γ mode. Results of fits of data to straight line are also shown.

correction for the presence of background 511-keV annihilation photons. The effect of virtually eliminating the deleterious effect of these photons was illustrated by the fact that the SI (Table 3) was very close to unity.

The results of the detection sensitivity measurements obtained for ^{18}F with the probe in the γ-optimized mode

revealed that the β-detection sensitivity increased marginally (7.8%) compared with that of the β mode. This increase was caused by the small detection cross-section of 511-keV photons in silicon ($\mu_{total} = 0.215$ cm^{-1}) compared with the very high detection efficiency for positrons. Even though the interaction cross-section for annihilation photons in the
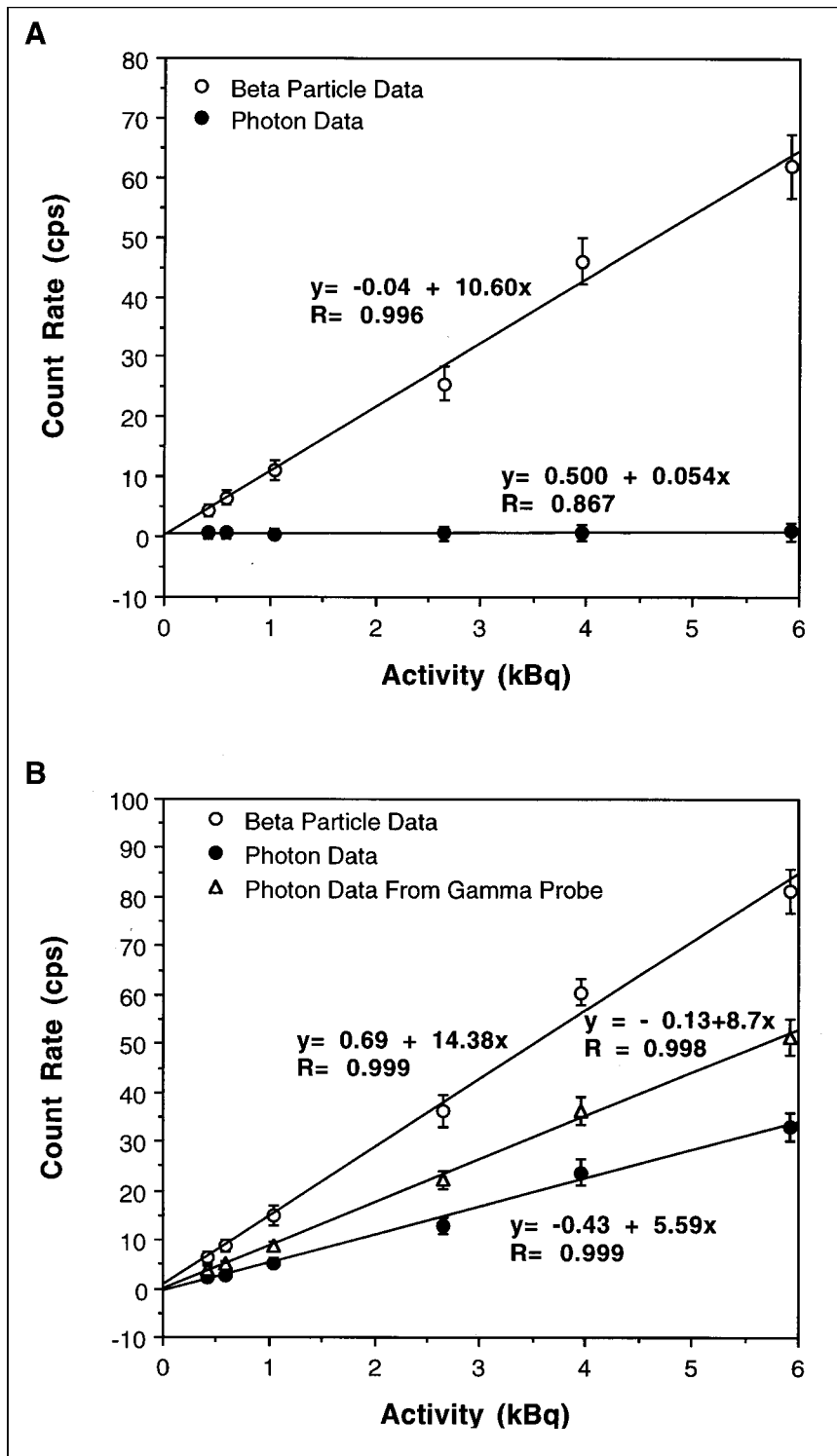
FIGURE 3. Results of sensitivity measurements for [99mTc] for two different acquisition modes. (A) β mode. (B) γ mode. Results of fits of data to straight line are also shown.

detectors was small, the photon-detection sensitivity increased substantially compared with the results acquired in β mode caused by the summation of signals from both detectors. The increased detected photon sensitivity caused a reduced SI compared with that in the β mode (Table 3).

Although [99mTc] is exclusively used in γ-imaging applications, a small percentage of its decays (8.7%) result in the emission of 119.4-keV conversion electrons (Table 1). Therefore, the β-detection sensitivity was significantly smaller than that measured for the pure β-emitting [18F] (Fig.
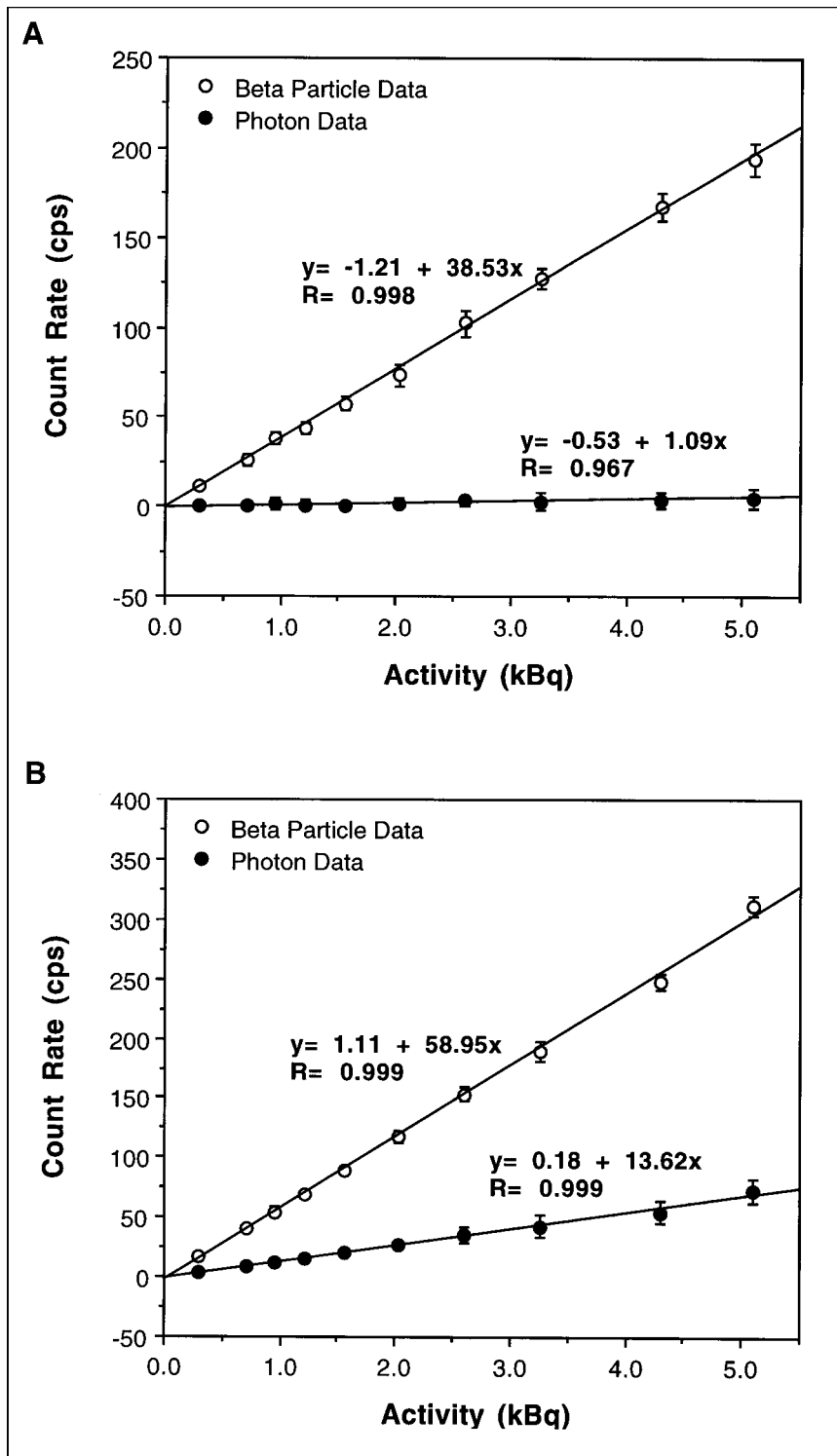
FIGURE 4. Results of sensitivity measurements for ^{111}In for two different acquisition modes. (A) β mode. (B) γ mode. Results of fits of data to straight line are also shown.

3). An additional factor affecting β sensitivity was the increased interaction probability of the 140-keV γ-rays in the IISDs (compared with the 511-keV annihilation photons). The total linear attenuation coefficient for 140-keV photons in silicon (μ_{total}) was 0.325 cm^{-1} compared with 0.215 cm^{-1} for 511-keV photons. More photons, therefore, were absorbed in the first detector. Thus, more of the γ-rays behaved like β particles, compared with annihilation photons. It was this phenomenon that caused the slightly increased photon detection sensitivity and lower SI compared

TABLE 2
Detection Sensitivity Results for Both Modes of Data Acquisition (β and γ)

Radionuclide	β Sensitivity (cps/kBq) in mode		Photon sensitivity (cps/kBq) in mode	
	β	γ	β	γ
[18]F	204.18 ± 3.12	220.06 ± 3.61	0.013 ± 1.05	16.58 ± 1.30
[99m]Tc	10.60 ± 0.68	14.38 ± 0.57	0.054 ± 0.24	5.59 ± 0.41
				8.75 ± 0.47*
[111]In	38.53 ± 1.16	58.95 ± 1.14	1.09 ± 0.66	13.62 ± 1.04

*Measurement made with Navigator γ probe (RMD, Inc.)

with [18]F. In γ-acquisition mode, the β sensitivity increased by ~36% compared to β-mode data, because of the addition of γ-ray events detected in the second detector. The photon sensitivity measured in this mode compared surprisingly well with the photon sensitivity measured with the specialized γ probe. Thus, it may be possible to use the dual, solid-state probe to aid in performing some sentinel node biopsies. The relatively high sensitivity for detecting γ-rays emitted by ^{99m}Tc and the relatively low β sensitivity resulted in the lowest SI calculated for any of the radionuclides tested (Table 3).

The use of ^{111}In for guidance of cancer surgeries is gaining interest, in part because of the variety of pharmaceuticals that can be labeled with this radionuclide. In addition to two γ-rays, ^{111}In emits two conversion electrons and several x-rays. The probe system was capable of detecting these emissions. In β mode, the β-detection sensitivity was relatively high compared with that measured for ^{99m}Tc, because of the detection of the conversion electrons as well as the γ- and x-rays (Fig. 4). As with the lower energy γ-rays emitted by ^{99m}Tc, more of the 171.3-keV ($\mu_{total} = 0.31$ cm^{-1}) and 245.0-keV ($\mu_{total} = 0.24$ cm^{-1}) x-rays were absorbed in the first detector compared with annihilation photons. In addition, the x-rays interacted almost exclusively with the first detector (the linear attenuation coefficients for these x-rays ranged from 4.6 to 6.0 cm^{-1}). The increased photon sensitivity and γ-ray-shielding effect of the first silicon wafer resulted in a reduced SI compared with measurements made with [18]F (Table 3). In γ mode, the β-detection sensitivity increased by 53% compared with data acquired in β mode. This significant increase was caused by the addition of the signals from the two γ-rays detected in the second wafer. Addition of these

events also produced increased photon sensitivity (Table 2) and reduced SIs (Table 3).

This investigation demonstrated the flexibility of the dual, solid-state intraoperative-probe system. The device was shown to be capable of detecting β and photon emissions produced by three commonly used radionuclides. The system's performance was not, however, equivalent for all radionuclides. This phenomenon was caused mostly by the nature of the emissions produced by each radionuclide. The flexibility of the system could perhaps allow the development of dual-radiopharmaceutical procedures. For example, FDG and ^{99m}Tc-sulfur colloid could be administered simultaneously to aid in guiding different aspects of breast cancer surgeries. Operated in β mode, the probe would be used to localize and guide the complete excision of the FDG-avid primary tumor. Indeed, a previous study using sham lesions and an anthropomorphic phantom demonstrated the potential of this system to localize tumor remnants after excision of the bulk tumor (12). FDG is perhaps the optimal choice for this purpose given its good targeting to breast carcinoma (18) and very good β-detection sensitivity and SI measured for ^{18}F with the probe in β-optimized mode (Tables 2 and 3). Identification of the sentinel node in the axilla could also be accomplished during the same surgical procedure by switching the probe into γ-optimized mode. The good detection sensitivity for 140-keV photons (Table 2) and the very high concentration of sulfur colloid in sentinel lymph nodes (26) compared with the concentration of FDG in normal tissues could allow the successful identification of the node in spite of the presence of FDG in the patient. Ultimately, however, the ability to identify sentinel nodes with this system can be confirmed only by testing this new procedure in a preclinical study.

The ability to operate the probe in two different acquisition modes, each suited for detection of β particles or photons, could be exploited to enhance the effectiveness of some currently used procedures. For example, in applications using ^{111}In-labeled pharmaceuticals, coarse and fine localization of tracer-avid lesions could be performed. Specifically, because the probe has good photon detection ca-

TABLE 3
Selectivity Results for Both Modes of Data Acquisition

Radionuclide	Selectivity index for mode	
	β	γ
[18]F	0.999936	0.924657
[99m]Tc	0.995283	0.611266
[111]In	0.976382	0.768957

pabilities in γ-optimized mode, gross localization of focal areas of increased tracer uptake would first be performed. Then the probe would be switched into β-optimized mode, which increases the SI index of the system, and used to more accurately identify localized areas of tracer-avid tumor using the detection of short-range conversion electrons. In this mode of operation, the probe could also be used to detect any tumor remnants left intact after the initial excision. One potential downside to using conversion electrons for lesion detection is their limited range in tissue. The 144.6- and 218.7-keV electrons emitted by ^{111}In have a range in tissue of between 0.5 and 0.75 mm. Therefore, only tracer present in tissue on the outer edges of a lesion is detectable. The degree to which this effect will limit the effectiveness of this procedure must ultimately be determined in a clinical study.

CONCLUSION

The results from this investigation demonstrated that the dual, solid-state probe system was capable of effectively detecting β particles and photons emitted by several different radionuclides. This capability could assist in improving existing methods and perhaps aid in the development of new methods for radionuclide-guided surgery.

ACKNOWLEDGMENTS

REFERENCES

1. Benevento A, Dominion L, Carcano G, Dionigi R. Intraoperative localization of gut endocrine tumors with radiolabeled somatostatin analogs and a gamma-detecting probe. *Semin Surg Oncol.* 1998;15:239–244.
2. Hinkle GH, Martin EW Jr. Intraoperative localization of neuroendocrine tumors with 125I-TYR(3)-octreotide and a hand-held gamma-detecting probe. *Surgery.* 1993;114:745–751.
3. Tuttle SE, Jewell SD, Mojzisik CM, et al. Intraoperative radioimmunolocalization of colorectal carcinoma with a hand-held gamma probe and MAb B72.3: comparison of in vivo gamma probe with in vitro MAb radiolocalization. *Int J Cancer.* 1988;15:352–358.
4. Muxi A, Pons F, Vidal-Sicart S, et al. Radioimmunoguided surgery of colorectal carcinoma with an ^{111}In-labeled anti-TAG72 monoclonal antibody. *Nucl Med Commun.* 1999;20:123–130.
5. Renda A, Iovino F, Capasso L, Ricciardelli L, Tammaro V, Acampa W. Radioimmunoguided surgery in colorectal cancer: a 6-year experience with four different technical solutions. *Semin Surg Oncol.* 1998;15:226–230.
6. Ahlman H. Radioisotope-guided surgery in patients with neuroendocrine tumours. *Digestion.* 1996;57(suppl 1):88–89.
7. Winzelberg GG, Grossman SJ, Rizk S, et al. Indium-111 monoclonal antibody B72.3 scintigraphy in colorectal cancer: correlation with computed tomography, surgery, histopathology, immunohistology, and human immune response. *Cancer.* 1992;69:1656–1663.
8. Curtet C, Vuillez JP, Daniel G, et al. Feasibility study of radioimmunoguided surgery of colorectal carcinomas using indium-111 CEA-specific monoclonal antibody. *Eur J Nucl Med.* 1990;17:299–304.
9. Davidson BR, Waddington W, Short MD, Boulos PB. Intraoperative localization of colorectal cancers using radiolabelled monoclonal antibodies. *Br J Surg.* 1991;78:664–670.
10. Saffer JR, Barrett HH, Barber HB, Woolfenden JM. Surgical probe design for a coincidence imaging system without a collimator. *Image Vis Comput.* 1992;10:333–341.
11. Daghighian F, Hoffman EJ, Shenderov P, Eshaghian B, Siegel S, Phelps MC. Intraoperative beta probe: a device for detecting tissue labeled with positron or electron emitting isotopes during surgery. *Med Phys.* 1994;21:153–175.
12. Raylman RR. A solid-state intraoperative beta probe system. *IEEE Trans Nucl Sci.* 2000;47:1696–1703.
13. MacDonald LR, Tornai MP, Levin CS, et al. Small area, fiber coupled scintillation camera for imaging beta-ray distributions intra-operatively. *Proc SPIE: Int Soc Opt Eng.* 1996;2551:92–101.
14. Tornai MP, MacDonald LR, Levin CS, Park J. Design considerations and initial performance of a 1.2 cm2 beta imaging intraoperative probe. *IEEE Trans Nucl Sci.* 1996;43:2326–2335.
15. Levin CS, Tornai MP, MacDonald LR, Hoffman EJ. Annihilation γ-ray background characterization and rejection for a small beta camera used for tumor localization during surgery. *IEEE Trans Nucl Sci.* 1997;44:1120–1126.
16. Tornai MP, Levin CS, MacDonald LR, et al. Development of a small area beta detecting probe for intra-operative tumor imaging [abstract]. *J Nucl Med.* 1995; 36(suppl):106P.
17. Coleman RE. PET in lung cancer. *J Nucl Med.* 1999;40:814–820.
18. Flanagan FL, Dehdashti F, Siegel BA. PET in breast cancer. *Semin Nucl Med.* 1998;28:290–302.
19. Delbeke D. Oncological applications of FDG PET imaging: brain tumors, colorectal cancer, lymphoma and melanoma. *J Nucl Med.* 199;40:591–603.
20. Hubner KF, McDonald TW, Niethammer JG, Smith GT, Gould HR, Buonocore E. Assessment of primary and metastatic ovarian cancer by positron emission tomography (PET) using 2-[18F]-deoxyglucose (2-[18F]FDG). *Gynecol Oncol.* 1993;51:197–204.
21. Keogan MT, Tyler D, Clark L, et al. Diagnosis of pancreatic carcinoma: role of FDG PET. *AJR.* 1998;171:1565–1570.
22. DeCicco C, Sideri M, Bartolomei M, et al. Sentinel node biopsy in early vulvar cancer. *Br J Cancer.* 2000;82:295–299.
23. Alex JC, Sasaki CT, Krag DN, Wenig B, Pyle PB. Sentinel lymph node radiolocalization in head and neck squamous cell carcinoma. *Laryngoscope.* 2000; 110:198–203.
24. Gogel BM, Kuhn JA, Ferry KM, et al. Sentinel lymph node biopsy for melanoma. *Am J Surg.* 1998;176:544–547.
25. Krag DN. Minimal access surgery for staging regional lymph nodes: the sentinel-node concept. *Curr Probl Surg.* 1998;35:951–1016.
26. Rubio IT, Korourian S, Cowan C, Krag DN, Colvert M, Klimberg VS. Sentinel lymph node biopsy for staging breast cancer. *Am J Surg.* 1998;176:532–537.